Chaos Control of Doubly-Fed Induction Generator via Delayed Feedback Control

Co Nhu Van

Department of Cybernetics, University of Transport and Communications, Vietnam | Institute for Control Engineering and Automation, Hanoi University of Science and Technology, Vietnam
vancn@utc.edu.vn

Nguyen Thanh Hai

Department of Electronic Engineering, University of Transport and Communications, Vietnam
nguyenthanhhai@utc.edu.vn
(corresponding author)

Nguyen Phung Quang

Institute for Control Engineering and Automation, Hanoi University of Science and Technology, Vietnam
quang.nguyenphung@hust.edu.vn

ABSTRACT

With the increasing wind power penetration, wind farms are directly influencing the power systems, so the need to improve the quality of the system is an open research topic. A Doubly-Fed Induction Generator (DFIG) is often used in wind power systems. However, DFIG has a complex structure and often works in harsh environments, so potential faults may occur. Faults can cause the system to fall into a chaotic working state, which is a harmful phenomenon for DFIG, since it makes the operating quality of the system worse, even leading to system destruction if not fixed on time. This study presents simulations of the chaotic phenomenon that occurs for a DFIG under specific working conditions based on Lyapunov's exponents. The delay feedback controller is designed, and along with the selection of the appropriate controller parameters, the chaotic phenomenon is quickly eliminated, bringing the system back to stable operation.

I. INTRODUCTION

Chaos can be beneficial as it may speed up chemical reactions, enhance mixing, provide a powerful mechanism for heat and mass transfer, etc. However, in many situations, chaos is an undesirable phenomenon, it can lead to increased mechanical fatigue for irregular oscillations, and non-convection energy absorption in a turbulent regime can lead to system parameters exceeding the safe level. Chaos is a phenomenon that only occurs in nonlinear systems, sensitive to initial conditions, and non-periodic but obeying certain laws. A dynamic system with chaotic motion needs to meet the following conditions [1-2]:

- The system has at least three independent variables.

- The equation of motion must have nonlinear terms. In addition, the phase space of the system must have a dimension of not less than 3 to ensure the existence of

divergent trajectories, be confined to a finite domain of the dynamics space, and ensure uniqueness of the orbit.

First of all, we need to note that in a linear dynamic system, chaos never occurs. So, when we talk about chaos, we mean nonlinear systems. However, not all nonlinear systems have chaotic motion. There are different methods of detecting chaos such as the Fourier analysis method, time responses, phase portraits, bifurcation diagram of the maximum value of the state variable over time, and calculations of Lyapunov exponents used to illustrate the chaotic behavior when changing the characteristic value. The main interest of this paper is focused on the Lyapunov exponent because it can be calculated with relative ease and it provides confirmation of the presence of chaos in the observed data [3]. When the average Lyapunov exponent is calculated as positive, it indicates chaotic behavior occurring in the system. From that, the chaotic working area of the object is drawn, and a control method is proposed to bring the system to a stable working state,

extinguishing the self-sustaining oscillations with high amplitude and abnormal changes.

Due to the harsh working environment of wind farms, the DFIG parameters can change with temperature, time, load conditions, etc. DFIG is prone to faults such as gearbox faults, power converter faults, stator winding faults, rotor winding faults, velocity sensor faults, etc. [4-7], from which the system may fall into a state of chaotic operation, leading to poor working quality, which can be the cause of problems and failures. Among electrical failures, insulation failures in the stator windings cause the majority (30%-40%) of induction machine failures, including DFIGs [8-10]. Although a DFIG has a complex structure, prone to failure, it is still the most used structure in wind power systems due to its outstanding advantages. Therefore, there have been many research works put forth to improve the quality and performance of the system [6, 11-16]. The research on bifurcation and chaos for the DFIG system is very limited [17-23] and does not cover all the potential risks. The above studies have shown that, under certain operating conditions, a DFIG can be chaotic. Authors in [18, 20] evaluate that phenomenon based on computer simulations but have not evaluated it on a solid theoretical basis, or do not give specific conditions on which parameter changes in the system lead to chaos [20]. Authors in [21] analyzed the phenomenon of chaos and presented several risks that make the DFIG system chaotic. On the basis of theoretical analysis (algorithm to test 0-1) and through simulation, authors in [23] evaluated the stability and chaos of the system. The study also gives specific conditions of the parameter set causing chaos for the DFIG, however the condition of 3 simultaneous faults (stator winding fault, rotor winding fault, and rotor speed sensor fault) rarely occurs in practice.

This study demonstrates that DFIG faces a chaotic phenomenon when the system parameters change in case of stator winding failure, based on theoretical analysis and simulations. From there, the delay response controller will be designed to eliminate chaos, return the system to stability and avoid possible risks.

II. MATHEMATICAL MODEL OF DFIG, CHAOS CONTROL, AND DELAY FEEDBACK CONTROL METHOD

A. Mathematical Model of DFIG

One of the main control objectives for the DFIG is the independent control of active and reactive power through decoupled control of rotor currents i_{rd} and i_{rq} [24]. The starting point for deducing the state-space model of the DFIG is the voltage equations for the stator and rotor windings [24-25]:

Stator voltage in stator winding system:

$$u_s^s = R_s \mathbf{i}_s^s + \frac{d\psi_s^s}{dt} \qquad (1)$$

Rotor voltage in rotor winding system:

$$u_r^r = R_r \mathbf{i}_r^r + \frac{d\psi_r^r}{dt} \qquad (2)$$

Rotor and stator flux:

$$\begin{cases} \psi_s = L_s \, \mathbf{i}_s + L_m \, \mathbf{i}_r \\ \psi_r = L_m \, \mathbf{i}_s + L_r \, \mathbf{i}_r \end{cases} \qquad (3)$$

where:

$$\begin{cases} L_s = L_m + L_{\sigma s} \\ L_r = L_m + L_{\sigma r} \end{cases}$$

Converting (1) and (2) to the dq coordinate system, for any internal rotation with angular speed ω_s we get:

$$\begin{cases} \mathbf{u}_s = R_s \mathbf{i}_s + \frac{d\psi_s}{dt} + j\omega_s \psi_s \\ \mathbf{u}_r = R_r \mathbf{i}_r + \frac{d\psi_r}{dt} + j\omega_r \psi_r \end{cases} \qquad (4)$$

where $\omega_s = \omega + \omega_r$

The generator stator is connected to the grid with constant voltage and frequency. Since the stator frequency is always identical to the grid frequency, the voltage drop across the stator resistor can be neglected in comparison with the voltage drop across the mutual inductance L_m and the dissipation inductance $L_{\sigma s}$ stator, which can be written as follows:

$$\mathbf{u}_s = R_s \mathbf{i}_s + \frac{d\Psi_s}{dt} => \mathbf{u}_s \approx \frac{d\Psi_s}{dt} \quad \text{or} \quad \mathbf{u}_s \approx j\omega_s \Psi_s \quad (5)$$

From (3), we obtain:

$$\mathbf{i}_s = \frac{1}{L_s}(\Psi_s - L_m \mathbf{i}_r)$$

$$\Psi_r = L_m \mathbf{i}_s + L_r \mathbf{i}_r$$

After suppressing the stator current $\mathbf{i}_s$ and the rotor flux Ψ_r, from system (4) we get:

$$\begin{cases} \frac{d\mathbf{i}_r}{dt} = -\frac{1}{\sigma}\left(\frac{1}{T_r} + \frac{1-\sigma}{T_s}\right)\mathbf{i}_r - j\omega_r \mathbf{i}_r \\ + \frac{1-\sigma}{\sigma}\left(\frac{1}{T_s} + j\omega\right)\Psi_s' + \frac{1}{\sigma L_r}\mathbf{u}_r + \frac{1-\sigma}{\sigma L_m}\mathbf{u}_s \qquad (6) \\ \frac{d\psi_s'}{dt} = \frac{1}{T_s}\mathbf{i}_r - \left(\frac{1}{T_s} + j\omega_s\right)\psi_s' + \frac{1}{L_m}\mathbf{u}_s \end{cases}$$

where $\psi_s' = \Psi_s/L_m$, $\sigma = 1 - L_m^2/(L_s L_r)$, $T_s = L_s/R_s$, $T_r = L_r/R_r$.

After decoupling both equations into real and imaginary components, we obtain the complete system of electrical equations of DFIG (7).

$$\begin{cases} \frac{di_{rd}}{dt} = -\frac{1}{\sigma}\left(\frac{1}{T_r} + \frac{1-\sigma}{T_s}\right)i_{rd} + \omega_r i_{rq} + \\ \quad \frac{1-\sigma}{\sigma}\left(\frac{1}{T_s}\Psi_{sd}' - \omega\Psi_{sq}'\right) + \frac{1}{\sigma L_r}u_{rd} - \frac{1-\sigma}{\sigma L_m}u_{sd} \\ \frac{di_{rq}}{dt} = -\frac{1}{\sigma}\left(\frac{1}{T_r} + \frac{1-\sigma}{T_s}\right)i_{rq} - \omega_r i_{rd} + \\ \quad \frac{1-\sigma}{\sigma}\left(\frac{1}{T_s}\Psi_{sq}' + \omega\Psi_{sd}'\right) + \frac{1}{\sigma L_r}u_{rq} - \frac{1-\sigma}{\sigma L_m}u_{sq} \qquad (7) \\ \frac{d\Psi_{sd}'}{dt} = \frac{1}{T_s}i_{rd} - \frac{1}{T_s}\Psi_{sd}' + \omega_s \Psi_{sq}' + \frac{1}{L_m}u_{sd} \\ \frac{d\Psi_{sq}'}{dt} = \frac{1}{T_s}i_{rq} - \frac{1}{T_s}\Psi_{sq}' - \omega_s \Psi_{sd}' + \frac{1}{L_m}u_{sq} \end{cases}$$

In grid voltage, the orientated coordinates are: $u_{sd} = u_s$, $\Psi_{sd}' = 0$, $\Psi_{sq}' = \Psi_s'$.

Summarizing the equation system (7) yields the following state space model for the DFIG in the grid voltage orientated reference frame (8):

$$\frac{d\mathbf{x}}{dt} = \mathbf{A}\mathbf{x} + \mathbf{B}_s\mathbf{u}_s + \mathbf{B}_r\mathbf{u}_r \qquad (8)$$

with: State vector $\mathbf{x}^T = \left[i_{rd}, i_{rq}, \Psi'_{sd}, \Psi'_{sq}\right]$, stator voltage vector $\mathbf{u}_s^T = \left[u_{sd}, u_{sq}\right]$, as the input vector on the stator side, and stator voltage vector $\mathbf{u}_r^T = \left[u_{rd}, u_{rq}\right]$ as the input vector on the rotor side.

The system matrix $\mathbf{A}$, the rotor input matrix $\mathbf{B}_r$ and the stator input matrix $\mathbf{B}_s$ may be written as:

$$\mathbf{A} = \begin{bmatrix} -\frac{1}{\sigma}\left(\frac{1}{T_r}+\frac{1-\sigma}{T_s}\right) & \omega_r & \frac{1-\sigma}{\sigma T_s} & -\frac{1-\sigma}{\sigma}\omega \\ -\omega_r & -\frac{1}{\sigma}\left(\frac{1}{T_r}+\frac{1-\sigma}{T_s}\right) & \frac{1-\sigma}{\sigma}\omega & \frac{1-\sigma}{\sigma T_s} \\ \frac{1}{T_s} & 0 & -\frac{1}{T_s} & \omega_s \\ 0 & \frac{1}{T_s} & -\omega_s & -\frac{1}{T_s} \end{bmatrix}$$

$$\qquad (9)$$

$$\mathbf{B}_s = \begin{bmatrix} -\frac{1-\sigma}{\sigma L_m} & 0 \\ 0 & -\frac{1-\sigma}{\sigma L_m} \\ \frac{1}{L_m} & 0 \\ 0 & \frac{1}{L_m} \end{bmatrix}; \quad \mathbf{B}_r = \begin{bmatrix} \frac{1}{\sigma L_r} & 0 \\ 0 & \frac{1}{\sigma L_r} \\ 0 & 0 \\ 0 & 0 \end{bmatrix}$$

B. Chaos Control and Delayed Feedback Control Method

Every parameter of the system has the potential to cause bifurcation and chaos, the idea of control is to bring these two properties towards its purpose, by adjusting the system parameters, or to hit the target by methods such system parameters transformation, changes in the structure of the system, input stimulus from outside, change the controller, or a control method based on the system's strange attractor set when a chaotic phenomenon occurs, bringing the trajectory to the target orbit with the new set parameter combination compatible with the old parameter. To do so, it is necessary to know the rate at which chaos or exponential growth increases and the oscillation amplitude of the system state variable. From there, a way to approach is by using accurate measurement equipment of system state variables and thus determining the stable and unstable working parameter areas, thereby determining the appropriate control method and the way to change the structure of the system if necessary. There are many methods of chaos control applied to electric drive systems and they have certain effects. The chaotic control method based on the delay feedback controller has been studied extensively [1, 26-30]. The delayed feedback control method, described in [31], is:

$$F(t) = K[y(t-\tau) - y(t)] = KD(t)$$

where τ is the delay time. If this time coincides with the period of ith periodic orbit $\tau = T_i$, i.e. $y(t) = y_i(t)$, it does not change the periodic orbits in the system. Choosing the appropriate

weight K of the feedback, we can achieve the stabilization of the system.

The delayed feedback control method is less complex and more responsive than other control methods. It allows for non-invasive stabilization in the sense that the control force disappears when the state has reached the target. Authors in [32] showed that the simple self-feedback delay controller gives better results than the sliding mode self-feedback delay controller when applied to control chaotic behavior in the IFOC of a 3-phase induction motor. Today, the DFC has become one of the most popular methods in chaos control research [33]. So far the number of published works on chaos control for DFIG is very limited and has not covered all the problems. To the best of our knowledge there are no works that apply DFC method to control the DFIG. This study aims to fill that gap.

III. CHAOTIC PHENOMENA AND CHAOS CONTROL FOR DFIG

A. Chaotic Behavior Analysis of DFIG

It can be seen from (7) that DFIG is a multivariable and nonlinear system (which is a necessary condition for a chaotic motion system). DFIG contains many parameters and the system works in harsh environments, therefore, the parameters can vary according to temperature, time, and system operating conditions. When the parameters of the system change, the system may appear to be chaotic. To clarify this issue, this study presents the chaotic phenomenon that occurs in DFIGs in cases of stator winding failure (this is the problem that accounts for the majority of electrical problems for DFIGs [8-10]). From the equation of motion of the rotor [6, 17], we combine with the first two equations of (7) to obtain a system of equations representing the rotor currents (i_{rd}, i_{rq}) and the rotor speed of DFIG as follows:

$$\begin{cases} \frac{di_{rd}}{dt} = -\frac{1}{\sigma}\left(\frac{1}{T_r}+\frac{1-\sigma}{T_s}\right)i_{rd} + (\omega_s - \omega)i_{rq} - \\ \qquad \frac{1-\sigma}{\sigma}\omega\frac{\Psi_s}{L_m} + \frac{1}{\sigma L_r}u_{rd} - \frac{1-\sigma}{\sigma L_m}u_s \\ \frac{di_{rq}}{dt} = -\frac{1}{\sigma}\left(\frac{1}{T_r}+\frac{1-\sigma}{T_s}\right)i_{rq} - (\omega_s - \omega)i_{rd} + \\ \qquad \frac{1-\sigma}{\sigma}\frac{1}{T_s}\frac{\Psi_s}{L_m} + \frac{1}{\sigma L_r}u_{rq} \\ \frac{d\omega}{dt} = \frac{3}{2}\frac{n_p^2 L_m \Psi_s}{J L_s}i_{rd} - \frac{D}{J}\omega - \frac{n_p}{J}T_L \end{cases} \quad (10)$$

From that, the structure diagram of the system is obtained as can be seen in [34], with: $x_1 = i_{rd}$; $x_2 = i_{rq}$; $x_3 = \omega$;

$$c_1 = -\frac{1}{\sigma}\left(\frac{1}{T_r}+\frac{1-\sigma}{T_s}\right); \ c_2 = \frac{1-\sigma}{\sigma L_m}\Psi_s; \ c_3 = \frac{1}{\sigma L_r}; \ c_4 = \frac{1-\sigma}{\sigma L_m};$$

$$c_5 = \frac{1-\sigma}{\sigma L_m T_s}\Psi_s; \ c_6 = \frac{3n_p^2 L_m \Psi_s}{2J L_s}; \ c_7 = \frac{D}{J}; \ c_8 = \frac{n_p}{J}.$$

Equation (10) will be abbreviated to:

$$\begin{cases} \dot{x}_1 = c_1 x_1 + (\omega_s - x_3)x_2 - c_2 x_3 \\ \qquad + c_3 u_{rd} - c_4 u_s \\ \dot{x}_2 = c_1 x_2 - (\omega_s - x_3)x_1 + c_5 + c_3 u_{rq} \\ \dot{x}_3 = c_6 x_1 - c_7 x_3 - c_8 T_L \end{cases} \quad (11)$$

The system's main parameters used in our simulations are listed in Table I [25].

TABLE I. MAIN PARAMETERS OF THE DFIG SYSTEM

Rated power (P)	1.5MW
Grid voltage (U)	690V
Grid frequency (f)	50 Hz
Moment of inertia (J)	2kgm^2
Pole pairs (n_p)	3
Damping coefficient (D)	0.001Nm/rad/s
Load torque (T_L)	3N.m
Stator resistance (R_s)	2.139mΩ
Stator inductance (L_s)	4.05mH
Rotor resistance (R_r)	2.139mΩ
Rotor inductance (L_r)	4.09mH
Mutual inductance(L_m)	4mH

From the structural model of the system above, simulations in MATLAB were conducted with the following algorithm: first, simulate with the system's parameter set in normal mode, and then, simulate the case of stator winding failure, in order to be able to clarify the stable working state of the system in normal mode and the system falling into a chaotic state when the parameters of the stator windings change.

In the normal operating mode, the simulation results show that the phase trajectories of i_{rd}, i_{rq} and ω oscillated at the beginning, but soon they stabilized (Figures 1 and 2). The results of calculating the Lyapunov exponent also show that all 3 Lyapunov exponents are negative (Figure 3). Thus, with a normal set of parameters, the system is stable.
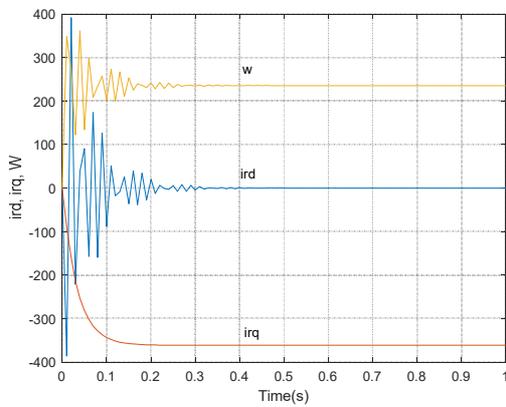

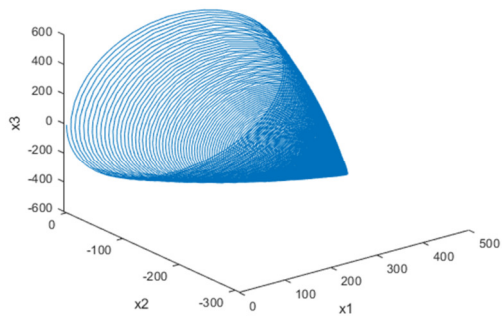Fig. 1. Time series diagrams of i_{rd}, i_{rq}, ω.

Fig. 2. Phase trajectory diagram x_1, x_2, x_3 (i_{rd}, i_{rq},ω).
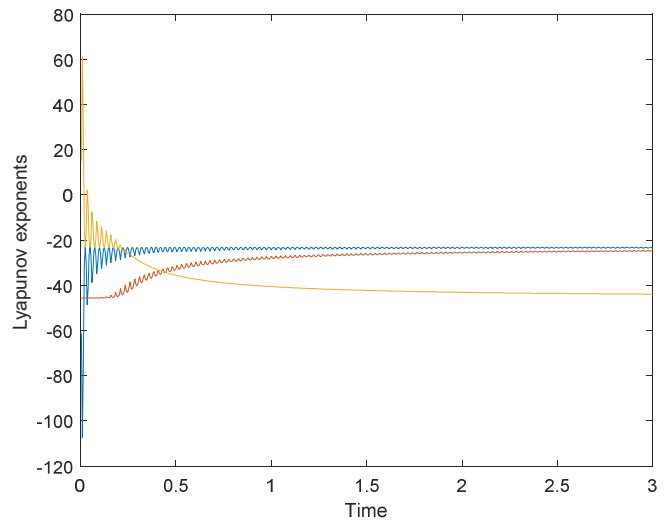

Fig. 3. Variation of Lyapunov's exponent over time when the system is operating under normal conditions.

When stator winding failures occur, the inductance of the coil changes to other values. Through the simulation on MATLAB with the variation of the inductance parameter of the stator winding, the results in Figures 4-7 show that the orbit is attracted to the basin of attraction, but it is not stable there. The phase orbit is confined, which is possible to approach arbitrarily close to some point of the basin of attraction, but never to repeat the same at a later point in time. At the same time, the results of calculating the Lyapunov exponent (Figure 8 and Table II) show that the system always has 2 positive Lyapunov's exponents. Thus, the DFIG system is chaotic.
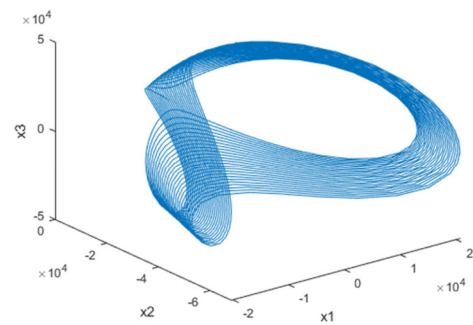

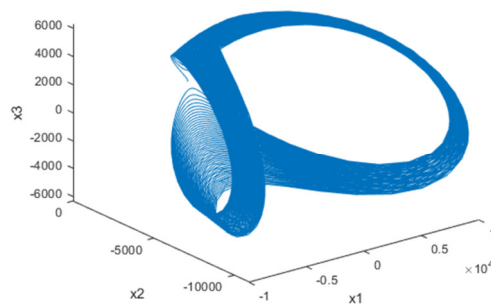Fig. 4. Phase trajectory diagram showing chaotic orbits at L_s = 3.8mH.

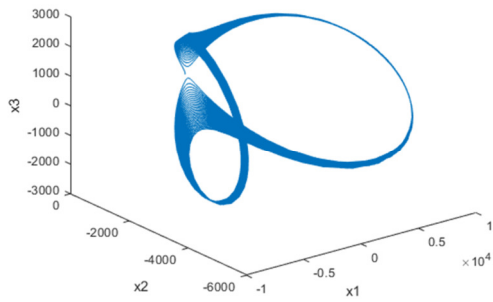Fig. 5. Phase trajectory diagram showing chaotic orbits at L_s = 3.3mH.

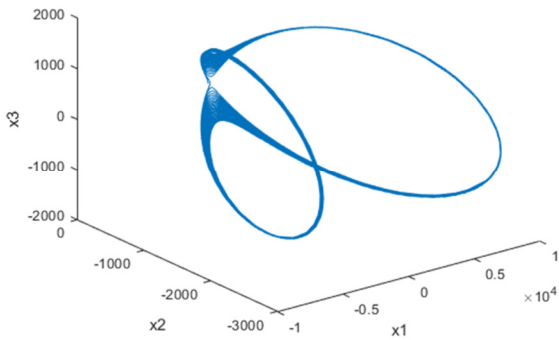Fig. 6.   Phase trajectory diagram showing chaotic orbits at L_s = 2.7 mH.

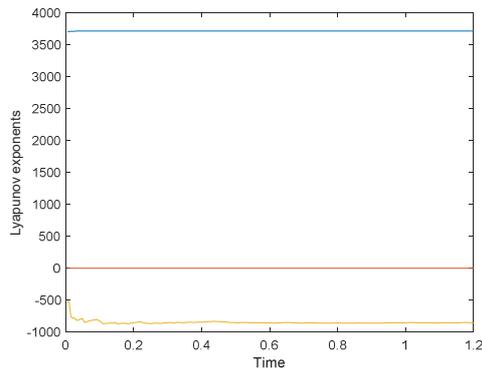Fig. 7.   Phase trajectory diagram showing chaotic orbits at L_s = 2.2mH.

Fig. 8.   Variation of Lyapunov's exponent over time when the system is chaotic.

TABLE II.   LYAPUNOV'S EXPONENT

Time	λ_1	λ_2	λ_3
0.05	3713.00	3.13	-794.31
0.15	3713.90	3.10	-862.60
0.25	3714.08	3.09	-866.10
0.35	3714.16	3.09	-848.98
0.45	3714.20	3.09	-831.52
0.55	3714.23	3.09	-852.85
0.65	3714.25	3.09	-849.68
0.75	3714.27	3.09	-859.42
0.85	3714.28	3.09	-858.06
0.95	3714.28	3.09	-854.43
1.00	3714.29	3.09	-852.66

B. Chaos Control for DFIG

As described above, the controller's structure aimed to eliminate the chaos that has occurred for DFIG is:

$$\begin{cases} \dot{x}_1 = c_1 x_1 + (\omega_s - x_3)x_2 - c_2 x_3 \\ \quad + c_3 u_{rd} - c_4 u_s + K_1[x_1(t - \tau_1) - x_1] \\ \dot{x}_2 = c_1 x_2 - (\omega_s - x_3)x_1 \\ \quad + c_5 + c_3 u_{rq} + K_2[x_2(t - \tau_2) - x_2] \\ \dot{x}_3 = c_6 x_1 - c_7 x_3 - c_8 T_L \end{cases} \quad (12)$$

where K_1, K_2 are the experimentally tunable weights of the perturbation. We provide the following operating schedule: When the system is chaotic, at 0.1s a delay feedback controller will be added to the system. The system achieved different results during the conducted simulations with different selected values of K_1, K_2 and τ_1, τ_2. The simulation results in Figure 8 with $K_1 = 22$, $K_2 = 25$, $\tau_1 = 0.001$, and $\tau_2 = 0.01$ show that the first time the phase trajectory of the system wanders in the confined space domain, then (when the controller is inserted) it is attracted to the equilibrium point and stabilizes there. Similarly, with different values of K_1, K_2, and τ_1, τ_2, the trajectory of x_1 in the time domain also shows that the stability of the system is different corresponding to the selected parameter set (Figures 9 to 14).
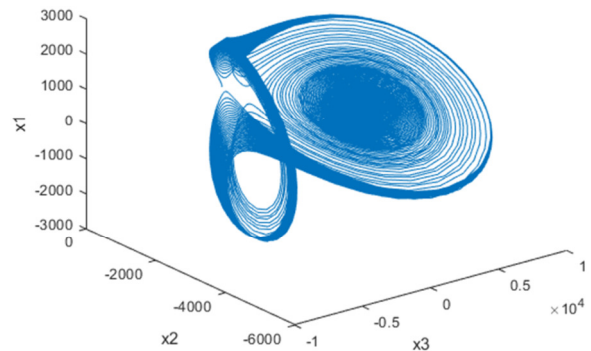

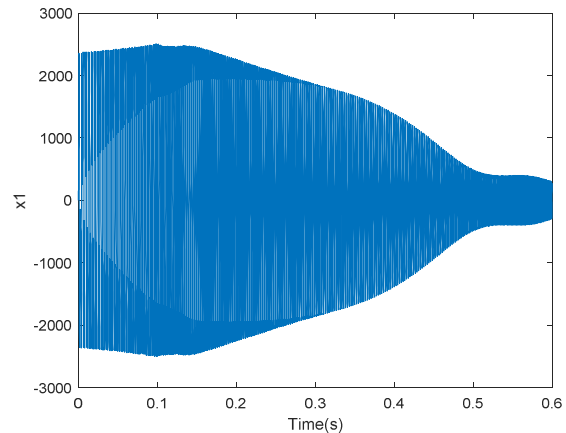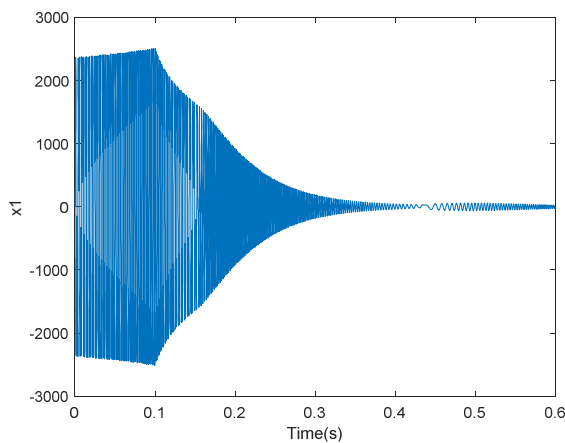Fig. 9.   Phase trajectory diagram between x_1, x_2 and x_3 with: K_1 =15, K_2=10, τ_1=0.001, τ_2=0.01.
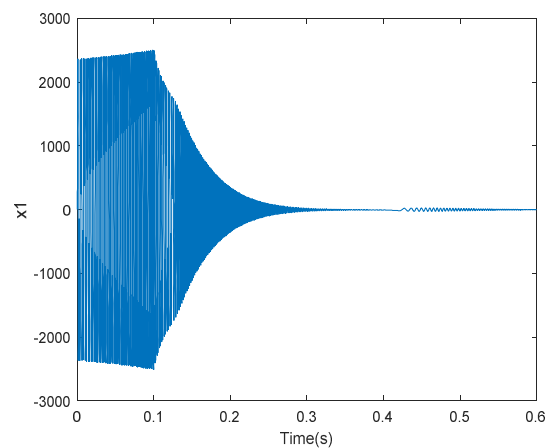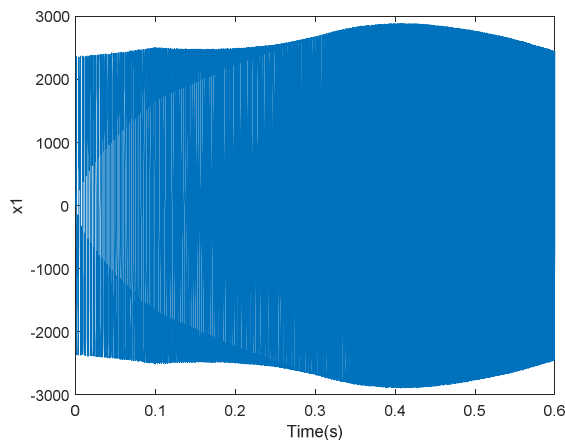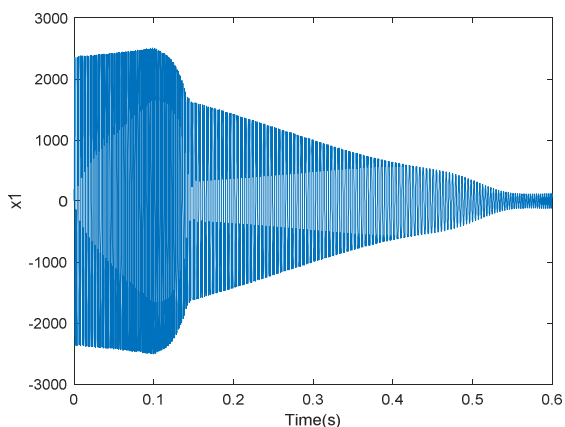

Fig. 10.   Time plot with K_1=15, K_2=10, τ_1=0.005, τ_2=0.0001

Fig. 11.   Time plot with K_1=15, K_2=10, τ_1=0.001, τ_2=0.0001

Fig. 12.   Time plot with K_1=15, K_2=10, τ_1=0.0001, τ_2=0.0001.

Fig. 13.   Time plot with K_1=25, K_2=10, τ_1=0.005, τ_2=0.0001.

The above simulation results show that, with the designed control law based on the delayed feedback control method, the system eliminated the chaotic phenomenon and returned to a stable state. By choosing the values of the appropriate parameters K_1, K_2, and τ_1, τ_2, the system will achieve optimum quality.

Fig. 14.   Time plot with K_1=25, K_2=10, τ_1=0.001, τ_2=0.0001

IV.   CONCLUSION

Chaos is harmful to DFIG. If this phenomenon is not detected and eliminated in time, the system's working quality will be poor, and the error can spread and cause great damage. This study has demonstrated the chaotic phenomenon that occurs for the DFIG when the stator winding is faulty, which is confirmed by calculating the Lyapunov exponent that always has two positive exponents, and simulation results show that the system has revealed the nature of chaos. This study proposes a control method to eliminate chaos for DFIG. The delay feedback control method is selected and designed. Before 0.1s, the curve shows strong fluctuations. At 0.1s a delay feedback controller was added to the system, the chaos was quickly eliminated, the system returns to stability, which can prevent further damage to the DFIG.

ACKNOWLEDGMENT

REFERENCES

[1]   K. T. Chau and Z. Wang, *Chaos in Electric Drive Systems: Analysis, Control and Application*. New York, NY, USA: Wiley, 2011.

[2]   N. V. Dao, T. K. Chi, and N. Dung, *Introduction to nonlinear dynamics and chaotic motion*. Hanoi, Vietnam: Vietnam National University Press, 2005.

[3]   M. Sajid, F. A. Almufadi, and M. Jahanzaib, "Chaotic Behavior in a Flexible Assembly Line of a Manufacturing System," *Engineering, Technology & Applied Science Research*, vol. 5, no. 6, pp. 891–894, Dec. 2015, https://doi.org/10.48084/etasr.611.

[4]   S. Karimi, A. Gaillard, P. Poure, and S. Saadate, "Current Sensor Fault-Tolerant Control for WECS With DFIG," *IEEE Transactions on Industrial Electronics*, vol. 56, no. 11, pp. 4660–4670, Aug. 2009, https://doi.org/10.1109/TIE.2009.2031193.

[5]   F. Cheng, Y. Peng, L. Qu, and W. Qiao, "Current-Based Fault Detection and Identification for Wind Turbine Drivetrain Gearboxes," *IEEE Transactions on Industry Applications*, vol. 53, no. 2, pp. 878–887, Mar. 2017, https://doi.org/10.1109/TIA.2016.2628362.

[6]   W. Yu, D. Jiang, J. Wang, R. Li, and L. Yang, "Rotor-current-based fault detection for doubly-fed induction generator using new sliding

mode observer," *Transactions of the Institute of Measurement and Control*, vol. 42, no. 16, pp. 3110–3122, Dec. 2020, https://doi.org/10.1177/0142331220941009.

[7] H. Ma, T. Chen, Y. Zhang, P. Ju, and Z. Chen, "Research on the fault diagnosis method for slip ring device in doubly-fed induction generators based on vibration," *IET Renewable Power Generation*, vol. 11, no. 2, pp. 289–295, 2017, https://doi.org/10.1049/iet-rpg.2016.0288.

[8] I. Idrissi, R. El Bachtiri, H. Chafouk, and M. Khanfara, "Fault Diagnosis of Stator Inter-Turn Short Circuit in Doubly Fed Induction Generator of Wind Turbine," in *6th International Conference on Control, Decision and Information Technologies*, Paris, France, Apr. 2019, pp. 1313–1318, https://doi.org/10.1109/CoDIT.2019.8820697.

[9] K. Ma, J. Zhu, M. Soltani, A. Hajizadeh, and Z. Chen, "Inter-Turn Short-Circuit Fault Ride-Through for DFIG Wind Turbines," *IFAC-PapersOnLine*, vol. 53, no. 2, pp. 12757–12762, Jan. 2020, https://doi.org/10.1016/j.ifacol.2020.12.1916.

[10] H. Mellah, S. Arslan, H. Sahraoui, K. E. Hemsas, and S. Kamel, "The Effect of Stator Inter-Turn Short-Circuit Fault on DFIG Performance Using FEM," *Engineering, Technology & Applied Science Research*, vol. 12, no. 3, pp. 8688–8693, Jun. 2022, https://doi.org/10.48084/etasr.4923.

[11] N. P. Quang, A. Dittrich, and A. Thieme, "Doubly-fed induction machine as generator : Control algorithms with decoupling of torque and power factor," *Electrical Engineering*, vol. 80, no. 5, pp. 325–335, 1997.

[12] N. P. Quang, "Review paper: General overview of control problems in wind power plants," *Journal of Computer Science and Cybernetics*, vol. 30, no. 4, pp. 313–334, Dec. 2014, https://doi.org/10.15625/1813-9663/30/4/5762.

[13] O. P. Bharti, R. K. Saket, and S. K. Nagar, "Controller Design For DFIG Driven By Variable Speed Wind Turbine Using Static Output Feedback Technique," *Engineering, Technology & Applied Science Research*, vol. 6, no. 4, pp. 1056–1061, Aug. 2016, https://doi.org/10.48084/etasr.697.

[14] P. D. Chung, "Voltage Enhancement on DFIG Based Wind Farm Terminal During Grid Faults," *Engineering, Technology & Applied Science Research*, vol. 9, no. 5, pp. 4783–4788, Oct. 2019, https://doi.org/10.48084/etasr.3117.

[15] A. Dountio Tchioffo, E. D. Kenmoe Fankem, G. Golam, M. Kamta, and J. Y. Effa, "Control of a BDFIG Based on Current and Sliding Mode Predictive Approaches," *Journal of Control, Automation and Electrical Systems*, vol. 31, no. 3, pp. 636–647, Jun. 2020, https://doi.org/10.1007/s40313-020-00566-z.

[16] A. Guediri and S. Touil, "Modeling and Comparison of Fuzzy-PI and Genetic Control Algorithms for Active and Reactive Power Flow between the Stator (DFIG) and the Grid," *Engineering, Technology & Applied Science Research*, vol. 12, no. 3, pp. 8640–8645, Jun. 2022, https://doi.org/10.48084/etasr.4905.

[17] L. Yang, X. Ma, and D. Dai, "Hopf bifurcation in doubly fed induction generator under vector control," *Chaos, Solitons & Fractals*, vol. 41, no. 5, pp. 2741–2749, Sep. 2009, https://doi.org/10.1016/j.chaos.2008.10.006.

[18] H. Xue and Y. Wang, "Fuzzy optimal control of doubly fed induction wind power generator systems," in *International Conference on Mechanic Automation and Control Engineering*, Wuhan, China, Jun. 2010, pp. 3512–3515, https://doi.org/10.1109/MACE.2010.5536699.

[19] L. H. Yang, Z. Xu, J. Ostergaard, Z. Y. Dong, and X. K. Ma, "Hopf bifurcation and eigenvalue sensitivity analysis of doubly fed induction generator wind turbine system," in *IEEE PES General Meeting*, Minneapolis, MN, USA, Jul. 2010, pp. 1–6, https://doi.org/10.1109/PES.2010.5590020.

[20] Z. Li, S.-C. Wong, C. K. Tse, and G. Chu, "Bifurcation in wind energy generation systems," *International Journal of Bifurcation and Chaos*, vol. 20, no. 11, pp. 3795–3800, Nov. 2010, https://doi.org/10.1142/S0218127410028070.

[21] Y. Yang, M. Zeng-Qiang, and L. Xing-Jie, "Analysis of chaos in doubly fed induction generator and sliding mode control of chaos synchronization," *Acta Physica Sinica*, vol. 60, no. 7, 2011, Art. no. 070509.

[22] D. Jiang, W. Yu, J. Wang, G. Zhong, and Z. Zhou, "Dynamic Analysis of DFIG Fault Detection and Its Suppression Using Sliding Mode Control," *IEEE Journal of Emerging and Selected Topics in Power Electronics*, vol. 11, no. 1, pp. 643–656, Oct. 2023, https://doi.org/10.1109/JESTPE.2020.3035205.

[23] C. N. Van, N. T. Hai, and N. P. Quang, "Wind power plants using doubly fed induction generator and the risk of chaos," presented at the The 6th International Conference and Exhibition on Control and Automation, Vietnam, 2022.

[24] N. P. Quang and J.-A. Dittrich, *Vector Control of Three-Phase AC Machines-System Development in the Practice*. New York, NY, USA: Springer, 2015.

[25] D. Xu, F. Blaabjerg, W. Chen, and N. Zhu, *Advanced Control of Doubly Fed Induction Generator for Wind Power Systems*. New York, NY, USA: John Wiley & Sons, 2018.

[26] K. Pyragas, "Control of Chaos via an Unstable Delayed Feedback Controller," *Physical Review Letters*, vol. 86, no. 11, pp. 2265–2268, Mar. 2001, https://doi.org/10.1103/PhysRevLett.86.2265.

[27] Y. Gao and K. T. Chau, "Chaotification of permanent-magnet synchronous motor drives using time-delay feedback," in *28th Annual Conference of the Industrial Electronics Society*, Seville, Spain, Nov. 2002, vol. 1, pp. 762–766, https://doi.org/10.1109/IECON.2002.1187603.

[28] S. Emiroglu and Y. Uyaroglu, "Time Delay Feedback Control based Chaos Stabilization in Current Mode Controlled DC Drive System," *International Journal of Engineering and Applied Sciences*, vol. 4, no. 10, Oct. 2017, Art. no. 257350.

[29] J. Sun, "Delay-dependent stability criteria for time-delay chaotic systems via time-delay feedback control," *Chaos, Solitons & Fractals*, vol. 21, no. 1, pp. 143–150, Jul. 2004, https://doi.org/10.1016/j.chaos.2003.10.018.

[30] K. Chakrabarty and U. Kar, "Bifurcation and control of chaos in Induction motor drives." arXiv, Oct. 24, 2014, https://doi.org/10.48550/arXiv.1410.6574.

[31] Y. Bolotin, A. Tur, and V. Yanovsky, *Chaos: Concepts, Control and Constructive Use*. Berlin, Germany: Springer, 2009.

[32] A. S. K. Tsafack, R. Kengne, A. Cheukem, J. R. M. Pone, and G. Kenne, "Chaos control using self-feedback delay controller and electronic implementation in IFOC of 3-phase induction motor," *Chaos Theory and Applications*, vol. 2, no. 1, pp. 40–48, Jun. 2020.

[33] E. Scholl and H. G. Schuster, *Handbook of Chaos Control*. Berlin, Germany: John Wiley & Sons, 2008.

[34] P. Q. Nguyen, *Matlab & Simulink for Automation Engineers*. Hanoi, Vietnam: Science and Technics Publishing House, 2004.